Modeling the Oxidation of Ebselen and Other Organoselenium Compounds Using Explicit Solvent Networks

Craig A. Bayse* and Sonia Antony

Department of Chemistry and Biochemistry, Old Dominion University, Hampton Boulevard, Norfolk, Virginia 23529

Received: March 1, 2009; Revised Manuscript Received: March 29, 2009

The oxidation of dimethylselenide, dimethyldiselenide, *S*-methylselenenyl-methylmercaptan, and truncated and full models of ebselen (*N*-phenyl-1,2-benzisoselenazol-3(2*H*)-one) by methyl hydrogen peroxide has been modeled using density functional theory (DFT) and solvent-assisted proton exchange (SAPE), a method of microsolvation that employs explicit solvent networks to facilitate proton transfer reactions. The calculated activation barriers for these systems were substantially lower in energy ($\Delta G^{\ddagger} + \Delta G_{solv} = 13$ to 26 kcal/mol) than models that neglect the participation of solvent in proton exchange. The comparison of two- and three-water SAPE networks showed a reduction in the strain in the model system but without a substantial reduction in the activation barriers. Truncating the ebselen model to *N*-methylisoselenazol-3(2*H*)-one gave a larger activation barrier than ebselen or *N*-methyl-1,2-benzisoselenazol-3(2*H*)-one but provided an efficient means of determining an initial guess for larger transition-state models. The similar barriers obtained for ebselen and Me_2Se_2 ($\Delta G^{\ddagger} + \Delta G_{solv} = 20.65$ and 20.40 kcal/mol, respectively) were consistent with experimentally determined rate constants. The activation barrier for MeSeSMe ($\Delta G^{\ddagger} + \Delta G_{solv} = 21.25$ kcal/mol) was similar to that of ebselen and Me_2Se_2 despite its significantly lower experimental rate for oxidation of an ebselen selenenyl sulfide by hydrogen peroxide relative to ebselen and ebselen diselenide. The disparity is attributed to intramolecular Se−O interactions, which decrease the nucleophilicity of the selenium center of the selenenyl sulfide.

Introduction

The essential trace element selenium functions biologically as a scavenger of reactive oxygen species and is of interest for the prevention of chronic diseases related to oxidative stress including cancer, cardiovascular disease, and arthritis.[1] Selenium is incorporated into antioxidant proteins such as glutathione peroxidase (GPx) to manage oxidative stress and prevent cellular damage and apoptosis.[2] Natural and synthetic mimics of GPx, such as selenomethionine and ebselen, catalyze the same overall reaction as the enzyme (Scheme 1)[3] and have been examined in clinical trials for the prevention of cancer[4] and stroke,[5] respectively. The selenides selenomethionine[6] and Se-methylselenocysteine are major selenium sources in many plant species[7] but have the disadvantage of being metabolized into toxic byproducts.[8] The synthetic, nontoxic compound ebselen is a well-known and well-studied small organoselenium mimic of GPx[9] belonging to a series of heterocycles in which selenium is bonded to nitrogen (selenenamide). Unlike the mechanism of GPx (Scheme 1), which is simple and well-understood,[10] the mechanisms for the selenide and selenenamide functionalities are more complex and difficult to characterize experimentally.[3] Understanding these mechanisms is important for the design of more effective chemopreventatives, and computational chemistry has become an increasingly important tool for understanding the properties of organoselenium GPx mimics.[11] However, modeling of the mechanisms of these compounds requires special consideration because of the involvement of aqueous phase proton exchange pathways.

SCHEME 1: Mechanism for Scavenging of Reactive Oxygen Species by Glutathione Peroxidase

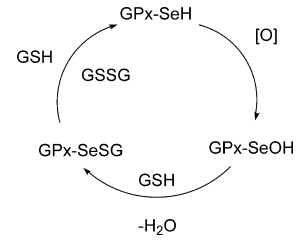

We have recently reported activation barriers for the GPx-like cycle of phenylselenol using networks of explicit solvent molecules as a means of facilitating proton transfer reaction.[12] We refer to this application of microsolvation as solvent-assisted proton exchange (SAPE). In our SAPE models, a limited number of solvent molecules connect the heavy atom proton donor and acceptor by a hydrogen-bonding network to provide a pathway for indirect proton exchange. Limiting the number of solvent molecules reduces the computational effort required to map the PES and reduces the conformations to a number manageable by a manual search. For these models, the path of reaction is necessarily concerted because the limited number of solvent molecules cannot adequately delocalize the accumulation of charge in the solvent cluster to allow for a charge-separated intermediate. Therefore, the proton exchange is simultaneous with heavy atom bond breaking/forming, and the concerted transition state derived from SAPE modeling is expected to be an upper bound to the activation barrier of the rate-determining step of the stepwise mechanism. SAPE results obtained for the GPx-like activity of PhSeH represented the first time that

* Corresponding author. E-mail: cbayse@odu.edu.

10.1021/jp901880n CCC: $40.75
Published on Web 04/17/2009

realistic activation barriers had been reported for the entire catalytic cycle of a small molecule GPx mimic.[12] The activation barriers were comparable both to the limited experimental information available for the enzyme as well as Morokuma's computational barriers for a truncated model of the GPx active site.[13]

1, R=Ph
3, R=Me

2

In this article, we examine the oxidation of several organoselenium compounds including the GPx mimic ebselen (*N*-phenyl-1,2-benzisoselenazol-3(2*H*)-one, **1**), two truncated ebselen models (*N*-methylisoselenazol-3(2*H*)-one, **2**, and *N*-methyl-1,2-benzisoselenazol-3(2*H*)-one, **3**), dimethyl selenide (Me_2Se, **4**), dimethyl diselenide (Me_2Se_2, **5**), and *S*-methylselenenyl-methylmercaptan (MeSeSMe, **6**) by methyl hydrogen peroxide (eq 1) using SAPE and density functional theory (DFT). The reaction pathways for the oxidation of these model GPx mimics are assumed to occur by transfer of an oxygen atom from MeOOH to the selenium center (eq 1).

$$RSeR' + MeOOH \rightarrow RSe(O)R' + MeOH \qquad (1)$$

The bond breaking/forming of the heavy atoms is accompanied by transfer of a proton from the hydroxyl group of MeOOH to O_{Me}. In protic solvents, this proton exchange is likely to be a stepwise process facilitated by acid/base catalysis by the bulk solvent. For example, the oxidation may be written as the two step process: (a) oxidation of the selenium center by heterolytic O−O bond cleavage with neutralization of the methoxide by removal of a proton from the bulk water and (b) deprotonation of the selenium oxide conjugate acid (eq 2). Note that the solvent water acts as a catalyst for the reaction by allowing the indirect proton exchange.

$$R_2Se + MeOOH + (H_2O)_n \rightarrow R_2Se{=}OH^+ + (OH^-)(H_2O)_{n-1} + MeOH \rightarrow R_2Se{=}O + (H_2O)_n + MeOH \qquad (2)$$

Quantum chemical modeling of this process as a direct proton exchange would be expected to produce activation barriers that are higher than experiment because of the omission of this catalytic role of bulk solvent. The activation barriers obtained using SAPE modeling for the oxidation of **1**−**6** by MeOOH presented below are lower than those obtained through direct proton transfer[14] and comparable to theoretical results for oxidation reactions of organoselenium compounds that occur without concomitant proton exchange.[15]

Theoretical Methods

DFT activation barriers for oxidation of MeSeH by MeOOH using a two-water SAPE network agree well with high-level ab initio methods when hybrid exchange−correlation (xc) functionals including 20−25% HF exchange are utilized.[11] Pure functionals and those with larger admixtures of HF exchange (i.e., BHandHLYP) tend to under- and overestimate activation barriers, respectively.[11] For the calculations in this study, geometry optimizations were performed using Gaussian 03[16] using the mPW1PW91[17] xc functional. Activation barriers obtained using this functional were comparable to those

SCHEME 2: SAPE Models for Oxidation of Organoselenium Compounds 1−6 Using (a) Two- and (b) Three-Water Networks

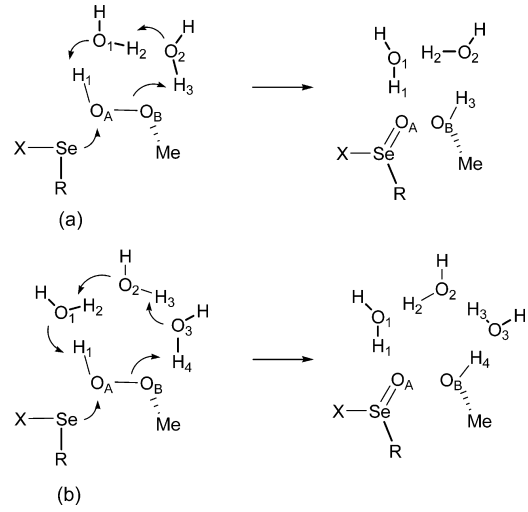

calculated at the MP2 and CCSD/MP2 levels. Selenium was represented by the Hurley et al.[18] relativistic effective core potential (RECP) double-ζ basis set augmented with a set of even-tempered s, p, and d diffuse functions. Oxygen was represented by Dunning's split-valence triple-ζ plus polarization function basis set (TZVP)[19] augmented with s- and p-type diffuse functions. Carbon basis sets were double-ζ plus polarization quality.[20] Hydrogens attached to noncarbon heavy atoms were TZVP quality, whereas those attached to carbon were double-ζ.

For the oxidation of **1**−**6** by the reaction in eq 1, transition states were obtained using two- and three-water SAPE networks (Scheme 2) by a manual scan of the Se−O_A bond formation coordinate from an initial reactant complex, followed by full refinement of the transition state structure. Each reactant complex was obtained by optimizing the geometry of the complex of the organoselenium compound with the lowest energy conformation of the two- or three-water−MeOOH cluster that connects the OH proton to the methoxy oxygen center by a hydrogen bonding network. Proton exchange through a single water molecule was not considered due to strain in the hydrogen-bonding interaction which is expected to lead to a higher activation barrier. In a similar DFT study of the epoxidation of ethylene, the one-water-assisted transition state was higher in energy than those obtained with larger SAPE networks.[21] All reported transition states were confirmed to have one imaginary frequency corresponding to the motion along the reaction coordinate connecting reactants and products. The reported energetics include zero-point energy (ZPE), thermal energy and enthalpy, and entropy corrections obtained at room temperature from the frequency calculation and bulk solvation effects in water calculated using the PCM model.[22]

Results and Discussion

In the following discussion, the stationary points are labeled by compound and number of waters in the SAPE network (e.g., $\mathbf{2}_{TS}^{3wat}$ is the transition state for the three-water model of **2**). The activation barriers and relative energies are listed in Table 1. Two simplified models of ebselen (**2** and **3**) were used to examine the effect of model truncation on the activation energies. Both models replaced the amide phenyl group with methyl. Model **2** also truncated the ring system to the simple

TABLE 1: Reaction Enthalpies (ΔH) and Solvation-Corrected Activation Gibbs Free Energies ($\Delta G^{\ddagger}$) and Solvation Corrections (ΔG_{solv}) for the Reduction of MeOOH by 1−6

		1		2		3	
n_{water}		TS	P	TS	P	TS	P
2	ΔH	16.35	−38.09	20.53	−35.79	16.51	−38.45
	$\Delta G^{\ddagger}$	20.20	−35.77	24.23	−32.68	19.07	−37.25
	$\Delta G^{\ddagger} + \Delta G_{solv}$	17.77	−37.60	17.88	−31.30	17.95	−37.69
3	ΔH	15.89	−38.21	19.22	−33.72	15.94	−38.87
	$\Delta G^{\ddagger}$	19.68	−36.45	23.55	−31.02	20.10	−36.51
	$\Delta G^{\ddagger} + \Delta G_{solv}$	20.65	−37.28	25.73	−30.21	21.25	−37.35

		4		5		6	
n_{water}		TS	P	TS	P	TS	P
2	ΔH	19.33	−36.95	23.17	−34.66	22.46	−36.72
	$\Delta G^{\ddagger}$	22.99	−35.84	24.79	−34.29	24.69	−36.03
	ΔG_{solv}	14.36	−41.42	17.66	−40.86	18.88	−40.80
3	ΔH	16.70	−34.83	19.66	−36.29	19.23	−38.19
	$\Delta G^{\ddagger}$	18.15	−35.97	23.44	−33.97	23.29	−35.35
	ΔG_{solv}	13.86	−44.53	20.40	−36.69	21.71	−36.93

TABLE 2: Evolution of the Critical Bond Distances along the Reaction Pathway and Imaginary Frequencies at the Transition State for Oxidation of Ebselen

	$\mathbf{1}^{2wat}$			$\mathbf{1}^{3wat}$		
	R	TS	P	R	TS	P
Se−N	1.892	1.930	1.904	1.890	1.918	1.909
O_A-O_B	1.432	2.073	3.054	1.433	2.000	3.021
$Se-O_A$	2.854	1.862	1.653	2.828	1.879	1.653
O_A-H_1	0.991	1.010	1.708	0.998	1.022	1.682
H_1-O_1	1.703	1.616	0.987	1.638	1.546	0.989
O_1-H_2	0.981	0.997	1.732	0.985	0.991	1.717
H_2-O_2	1.779	1.635	0.983	1.716	1.676	0.984
O_2-H_3	0.969	1.014	1.760	0.980	0.990	1.712
$H_3-O_{3/B}$	1.965	1.557	0.979	1.767	1.685	0.985
O_3-H_4				0.974	1.022	1.727
H_4-O_B				1.830	1.529	0.983
$Se-O_B$			2.686			2.607
ν_{TS}, cm^{-1}		88*i*			206*i*	

isoselenazolone. This model was used for the initial scan of the potential energy surface to determine the first estimate of the transition state. $SeMe_2$ serves as a model for redox-active selenoamino acids such as selenomethionine, Se-methylselenocysteine, and related Se-substituted selenocysteines for which we have recently published reports.[23,24]

The evolution of bond distances from reactant complex to transition state to product complex for ebselen is shown in Table 2. The geometries of the reactant complexes $\mathbf{1}_R^{2wat}$ and $\mathbf{1}_R^{3wat}$ (Figure 1) optimize to donor−acceptor complexes of the water−MeOOH cluster with ebselen arranged such that the lone pair of O_A can donate electron density to the Se−N antibonding MO.[25] For each of these models, the TS occurs when the $Se-O_A$ distance has decreased by 0.9 Å and the O_A-O_B distance has increased by 0.64 ($\mathbf{1}_{TS}^{2wat}$) and 0.57 Å ($\mathbf{1}_{TS}^{3wat}$). The O−O distances are comparable to values obtained with two-water SAPE networks for the epoxidation of ethylene[21] and oxidation of PhSeH,[12] both of which are reported as 1.928 Å. The imaginary modes for both $\mathbf{1}_{TS}^{2wat}$ and $\mathbf{1}_{TS}^{3wat}$ show significant motion in the SAPE networks in addition to heavy-atom bond forming/breaking with the largest for the protons transferring to/from the peroxide oxygen centers. The extra water in $\mathbf{1}_R^{3wat}$ allows a closer contact between the terminal water proton and O_B (1.873 vs 1.953 Å). The larger O_B-H_3 distance in $\mathbf{1}_R^{2wat}$ suggests that the hydrogen-bond connectivity is strained in $\mathbf{1}_R^{2wat}$, and a greater negative charge must be generated on the evolving methoxide to drive the proton exchange through the network. As a result, the greatest displacement from the reactant complex was for the formation of the methanol OH bond ($\Delta d(O_B-H_3)$ = 0.40 Å and $\Delta d(O_B-H_4)$ = 0.35 Å), and the heavy atoms must move further along the reaction pathway to reach the transition state. Nevertheless, the activation barrier for $\mathbf{1}_{TS}^{2wat}$ is only slightly higher than that for $\mathbf{1}_{TS}^{3wat}$ (Table 1). The product complexes $\mathbf{1}_P^{2wat}$ and $\mathbf{1}_P^{3wat}$ are exothermic (ΔH = −33 to −39 kcal/mol) and include the Se-oxide of the parent isoselenazolone, which is consistent with experimental monitoring of the reaction by ^{77}Se NMR.[26] (Note that a recent report shows that the seleninic acid ($RSeO_2H$) is the H_2O_2 oxidation product of ebselen because of hydrolysis of the Se−N bond.[27]) The product SAPE networks are arranged such that the methanol forms a donor−acceptor complex with the Se−N bond (Δd(Se−O) = 2.6 to 2.8 Å).

Similar descriptions of the reaction pathway may be obtained for the truncated models **2** and **3**, selected bond distances for which are given in Table 3. Although the bond distances for $\mathbf{2}_{TS}^{3wat}$, $\mathbf{3}_{TS}^{2wat}$, and $\mathbf{3}_{TS}^{3wat}$ are similar to the full ebselen model, the geometric parameters for the two-water model indicate that $\mathbf{2}_{TS}^{2wat}$ is shifted further along the reaction pathway. For this transition state, the O_A-O_B distance is ∼0.15 Å longer, and the O−H bonds being formed in the SAPE network as a part of the proton exchange occur at significantly shorter bond distances than the two-water transition states for **1** and **3**. Both these structural differences and the higher activation generally obtained for model **2** are attributed to the loss of electronic effects due to the truncation of the ring system to isoselenazolone. The similar activation barriers for **1** and **3** (Table 1) with either model suggest that the amide R group is less important to the energies than the benzisoselenazolone ring system.

The uncorrected activation Gibbs free energies ($\Delta G^{\ddagger}$) generally show that the size of the water network has little effect on the activation barrier. The difference between the two- and three-water activation barriers is generally <1 kcal/mol. Correcting for bulk solvation at the PCM level ($\Delta G^{\ddagger} + \Delta G_{solv}$, Table 1) tends to lower the activation barrier of the two-water models and increase the barriers of the three-water networks. It is somewhat counterintuitive that a larger model would result in an overall higher barrier, especially in light of the strain in the two-water network discussed above. However, the trend in the solvation-corrected barriers may be treated with some suspicion given that the solvent reaction field correction neglects hydrogen bonding interactions between the bulk solvent and the model system. Whether corrected or uncorrected, the activation barriers are substantially lower than DFT models in which the role of solvent in proton transfer reactions is not taken into account (i.e., ebselen: B3PW91/6-311++g(3df/3dp)//B3PW91/6-311 g(2df,p) 56.7 kcal/mol)[14] but are similar to the results for oxidation of the unsubstituted benzisoselenazol-3(2*H*)-one model of ebselen by peroxynitrite (B3LYP/6-311+g**: 14.8 kcal/mol) and peroxynitrous acid (B3LYP/6-311+g**: 14.4 kcal/mol).[15a,b]

Activation barriers and structural parameters for $SeMe_2$ (**4**), Me_2Se_2 (**5**), and MeSeSMe (**6**) are reported in Table 1 and Table 4/Figure 2, respectively. Many of the same observations about the differences in the energetics and structures in the two- and three-water SAPE models as were noted for ebselen (vide supra) may be made for these species and are not described in detail. The solvation-corrected SAPE activation barriers for $\mathbf{4}_{TS}^{2wat}$ and $\mathbf{4}_{TS}^{3wat}$ (14.4 and 13.9 kcal/mol) are similar to the $\Delta G^{\ddagger} + \Delta G_{solv}$ values reported by Musaev et al. for peroxynitrite-mediated

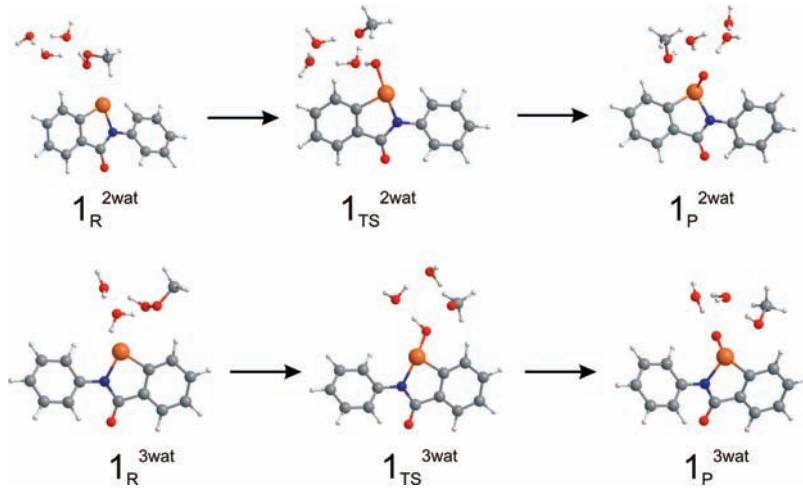

Figure 1. Transition state structures for the two- and three-water SAPE transition states for the oxidation of ebselen (**1**) by MeOOH. Selected bond distances are listed in Table 2.

TABLE 3: Selected Bond Distances and the Imaginary Frequencies of the Transition States for the Oxidation of Models 1 and 2

	$\mathbf{2}_{TS}^{2wat}$	$\mathbf{2}_{TS}^{3wat}$	$\mathbf{3}_{TS}^{2wat}$	$\mathbf{3}_{TS}^{3wat}$
Se−N	1.878	1.908	1.885	1.900
O_A−O_B	2.204	2.043	1.984	1.990
Se−O_A	1.815	1.883	1.902	1.890
O_A−H_1	1.019	1.006	1.020	1.019
H_1−O_1	1.579	1.640	1.560	1.561
O_1−H_2	1.012	0.995	0.982	0.991
H_2−O_2	1.562	1.649	1.758	1.680
O_2−H_3	1.047	1.011	0.984	0.990
H_3−$O_{3/B}$	1.448	1.571	1.743	1.687
O_3−H_4			1.014	1.021
H_4−O_B			1.574	1.533
ν_{TS}, cm^{-1}	139*i*	202*i*	97*i*	218*i*

TABLE 4: Selected Bond Distances (Angstroms) and the Imaginary Frequencies of the Transition States for the Oxidation of Dimethylselenide (4), Dimethyldiselenide (5), and MeSeSMe (6)

	$\mathbf{4}_{TS}^{2wat}$	$\mathbf{4}_{TS}^{3wat}$	$\mathbf{5}_{TS}^{2wat}$	$\mathbf{5}_{TS}^{3wat}$	$\mathbf{6}_{TS}^{2wat}$	$\mathbf{6}_{TS}^{3wat}$
Se_A−Se_B/S			2.409	2.411	2.282	2.289
O_A−O_B	1.934	1.895	1.904	1.892	1.910	1.897
Se_A−O_A	2.091	2.118	1.993	2.001	1.974	1.976
O_A−H_1	0.982	0.982	0.996	0.995	0.998	0.998
H_1−O_1	1.885	1.834	1.702	1.719	1.688	1.691
O_1−H_2	0.997	0.987	0.987	0.989	0.988	0.990
H_2−O_2	1.642	1.701	1.713	1.687	1.711	1.683
O_2−H_3	1.021	0.996	1.003	0.991	1.003	0.991
H_3−$O_{3/B}$	1.520	1.646	1.611	1.667	1.614	1.668
O_3−H_4		1.021		1.004		1.003
H_4−O_B		1.533		1.594		1.600
ν_{TS}, cm^{-1}	299*i*	263*i*	202*i*	213*i*	218*i*	235*i*

oxidation at the DFT(B3LYP/6-311+G**) level (11.7 kcal/mol from the reactant complex, 18.2 kcal/mol from separated reactants).[15c] SAPE modeling produces activation barriers for Me_2Se_2 ($\mathbf{5}_{TS}^{2wat}$ and $\mathbf{5}_{TS}^{3wat}$) that are slightly higher than those for ebselen, whereas recent gas-phase non-SAPE studies of the oxidation of ebselen and its derivatives find that the barrier for the diselenide derivative of ebselen is ~20 kcal/mol lower than that for ebselen itself.[14] Our result is qualitatively consistent with the kinetic data of Morgenstern et al.,[28] from which a difference of <0.1 kcal/mol in its Arrhenius activation energy can be calculated if the pre-exponential factors are assumed to be similar.

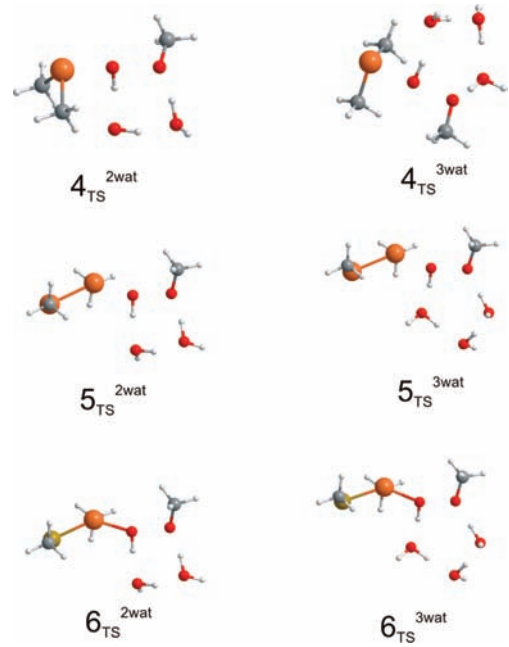

Figure 2. Transition state structures for the two- and three-water SAPE transition states for the oxidation of Me_2Se (**4**), Me_2Se_2 (**5**), and MeSeSMe (**6**) by MeOOH. Selected bond distances are listed in Table 4.

The transition states for **4**−**6** (Table 4) are found at shorter O_A−O_B distances (~1.90 Å) and longer Se−O_A distances (1.97 to 2.1 Å) than the selenenamide models. These differences can be attributed to the greater nucleophilicity of the low-oxidation-state selenium centers of **4**−**6**. Treating the reaction as the attack of selenium on an electrophilic OH^+ fragment to displace MeO^-, the longer O−O distances in the transition states for **1**−**3** show that this bond must be more activated for the high-oxidation-state selenenamide to attack. Despite these considerations, the activation barriers (Table 1) for oxidation of **4**−**6** are slightly higher than those for ebselen because of the greater potential for oxidation of Se^{II} to Se^{IV}. The product complexes of **4**−**6** are similar in exothermicity to the isoselenazolones ($\Delta H = -34$ to 38 kcal/mol). The two-water product complex $\mathbf{4}_P^{2wat}$ has a close interaction between the methanol and the selenium center but with an interaction with the Se−C rather than

the Se═O bond. The SAPE network is too short to allow the latter interaction without disrupting hydrogen bonding. The oxidative product of Me_2Se_2 is the asymmetric molecule MeSeSe(O)Me, as found by Pearson and Boyd.[14] The optimized product complexes $\mathbf{5}_P{}^{2wat}$ and $\mathbf{5}_P{}^{3wat}$ have the methanol molecule oriented to interact with the Se(O)−Se bond.

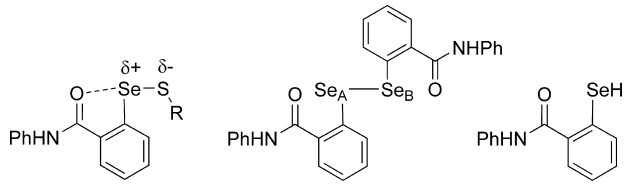

7 **8** **9**

The transition states for **5** and **6** are structurally similar (Table 4) with PCM-corrected activation Gibbs free energies for the selenenyl sulfide only 1 kcal/mol higher in energy than the diselenide analogues and the uncorrected $\Delta G^{\ddagger}$ roughly equal. This result is surprising given the slow rate of oxidation of the selenenyl sulfide (**7**) derivative of ebselen in comparison to that of **1**, ebselen diselenide (**8**), and ebselen selenol (**9**) (second-order rate constants are $\leq$0.01, 0.29, 0.32, and 2.8 mM^{-1} min^{-1}, respectively).[28] Qualitative observations determined through the monitoring of these reactions by ^{77}Se NMR are also consistent with these relative rates; selenenamides and the diselenide are rapidly oxidized, whereas the selenenyl sulfide reaction is slow.[29] (Note that the diselenide and selenenyl sulfide derivatives of ebselen cyclize to the selenenamide Se-oxides with elimination of the RSe or RS group.[26]) Mugesh has suggested that the overall low reactivity of ebselen may be due to the donation of electron density from the amide carbonyl to the Se−S bond of the selenenyl sulfide intermediate **7**.[29] In terms of the GPx-like mechanism for ebselen selenol **9** (analogous to GPx in Scheme 1), such an intramolecular interaction would increase the partial charge of the sulfur center to favor thiol exchange at selenium and disrupt the catalytic cycle rather than attack and reduction at sulfur. In terms of the oxidation of **7**, donation from the carbonyl oxygen decreases the nucleophilicity of selenium to prevent oxidation.

Conclusions

As shown for PhSeH and models of other chemical processes, inclusion of explicit solvent molecules is necessary to obtain reasonable activation barriers for proton-exchange processes in protic solvents. Variation in the activation barriers with the number of water molecules is less than 2 kcal/mol, which is in contrast with our results for the reduction of phenylselenenic acid (PhSeOH + MeSH → PhSeSMe + H_2O) in ref 12, where a four-water network relieved strain at the transition state to reduce the uncorrected $\Delta G^{\ddagger}$ by 10 kcal/mol (4.5 kcal/mol after solvation correction). In that case, the SAPE network connected heavy atoms from different molecules in the cluster, specifically, the thiol sulfur and the selenenic acid oxygen centers. The two-water network was more strongly anchored to the acidic SeOH proton such that the thiol was prevented from adopting an optimal angle for nucleophilic attack on the selenium center (162°). Increasing the size of the SAPE network to four and arranging the square water cluster for proton transfer between opposite corners allowed a better orientation of the thiol for backside attack (172°). In contrast, for the oxidation of **1**−**6**, the proton exchange is internal to the MeOOH molecule and is effectively independent of the orientation of the reacting fragments. Increasing the SAPE network for these systems better accommodates the proton transfer but only stabilizes the transition state by less than 2 kcal/mol. Comparison of the results for **1**−**3** shows that the choice of model is important to the activation barriers. Truncation of the ring system of ebselen increases the estimate of the activation barrier by several kcal/mol, whereas replacement of the *N*-Ph with methyl is within 1 kcal/mol of the full ebselen model. Nonetheless, the truncated models have value for rapid scan of the potential energy surface. The results for **1**−**3** are consistent with recent work by Mugesh,[30] which shows similar activities for the N-substitution of ebselen, and suggests that the benzisoselenazolone ring system is the preferred location for substitutions designed to modify the reactivity of ebselen.

Acknowledgment. We thank the Thomas F. Jeffress and Kate Miller Jeffress Memorial Trust and the National Science Foundation (CHE-0750413) for support of this research.

References and Notes

(1) (a) Ganther, H. E. *Carcinogenesis* **1999**, *20*, 1657. (b) Nordberg, J.; Arner, E. S. J. *Free Radical Biol. Med.* **2000**, *31*, 1287. (c) *Selenium: Its Molecular Biology and Role in Human Health*; Hatfield, D. L., Berry, M. J., Gladyshev, V. N., Eds.; Springer: New York, 2006. (d) Kayanoki, Y.; Fujii, J.; Islam, K. N.; Suzuki, K.; Kawata, S.; Matsuzawa, Y.; Taniguchi, N. *J. Biochem.* **1996**, *119*, 817. (e) Rayman, M. P. *Lancet* **2000**, *356*, 233. (f) Ghose, A.; Fleming, J.; Harrison, P. R. *BioFactors* **2001**, *14*, 127. (g) Tapiero, H.; Townsend, D. M.; Tew, K. D. *Biomed. Pharmacother.* **2003**, *57*, 134.

(2) Gromer, S.; Eubel, J. K.; Lee, B. L.; Jacob, J. *Cell. Mol. Life Sci.* **2005**, *62*, 2414.

(3) (a) Mugesh, G.; Singh, H. B. *Chem. Soc. Rev.* **2000**, *29*, 347. (b) Mugesh, G.; du Mont, W.-W.; Sies, H. *Chem. Rev.* **2001**, *101*, 2125.

(4) Lippman, S. M.; Goodman, P. J.; Klein, E. A.; Parnes, H. L.; Thompson, I. M.; Kristal, A. R.; Santella, R. M.; Probstfield, J. L.; Moinpour, C. M.; Albanes, D.; Taylor, P. R.; Minasian, L. M.; Hoque, A.; Thomas, S. M.; Crowley, J. J.; Gaziano, J. M.; Stanford, J. L.; Cook, E. D.; Fleshner, N. E.; Lieber, M. M.; Walther, P. J.; Khuri, F. R.; Karp, D. D.; Schwartz, G. G.; Ford, L. G.; Coltman, C. A. *J. Natl. Cancer Inst.* **2005**, *97*, 94.

(5) Lapchak, P. A.; Zivin, J. A. *Stroke* **2003**, *34*, 2013.

(6) Walter, R.; Roy, J. *J. Org. Chem.* **1971**, *36*, 2561.

(7) Arnault, I.; Auger, J. *J. Chromatogr., A* **2006**, *1112*, 23.

(8) Ganther, H. E.; Lawrence, J. R. *Tetrahedron* **1997**, *53*, 12299.

(9) Schewe, T. *Gen. Pharmacol.* **1995**, *26*, 1152.

(10) Gettins, P.; Crews, B. C. *J. Biol. Chem.* **1991**, *266*, 4804.

(11) Bayse, C. A.; Antony, S. *Main Group Chem.* **2007**, *6*, 185, and references therein.

(12) Bayse, C. A. *J. Phys. Chem. A* **2007**, *111*, 9070.

(13) Prabhakar, R.; Vreven, T.; Morokuma, K.; Musaev, D. G. *Biochemistry* **2005**, *44*, 11864.

(14) Pearson, J. K.; Boyd, R. J. *J. Phys. Chem A* **2006**, *110*, 8979.

(15) (a) Musaev, D. G.; Geletti, Y. V.; Hill, C. L.; Hirao, K. *J. Am. Chem. Soc.* **2003**, *125*, 3877. (b) Musaev, D. G.; Hirao, K. *J. Phys. Chem. A* **2003**, *107*, 1563. (c) Musaev, D. G.; Geletii, Y. V.; Hill, C. L. *J. Phys. Chem. A* **2003**, *107*, 5862.

(16) Frisch, M. J.; Trucks, G. W.; Schlegel, H. B.; Scuseria, G. E.; Robb, M. A.; Cheeseman, J. R.; Montgomery, J. A., Jr.; Vreven, T.; Kudin, K. N.; Burant, J. C.; Millam, J. M.; Iyengar, S. S.; Tomasi, J.; Barone, V.; Mennucci, B.; Cossi, M.; Scalmani, G.; Rega, N.; Petersson, G. A.; Nakatsuji, H.; Hada, M.; Ehara, M.; Toyota, K.; Fukuda, R.; Hasegawa, J.; Ishida, M.; Nakajima, T.; Honda, Y.; Kitao, O.; Nakai, H.; Klene, M.; Li, X.; Knox, J. E.; Hratchian, H. P.; Cross, J. B.; Bakken, V.; Adamo, C.; Jaramillo, J.; Gomperts, R.; Stratmann, R. E.; Yazyev, O.; Austin, A. J.; Cammi, R.; Pomelli, C.; Ochterski, J. W.; Ayala, P. Y.; Morokuma, K.; Voth, G. A.; Salvador, P.; Dannenberg, J. J.; Zakrzewski, V. G.; Dapprich, S.; Daniels, A. D.; Strain, M. C.; Farkas, O.; Malick, D. K.; Rabuck, A. D.; Raghavachari, K.; Foresman, J. B.; Ortiz, J. V.; Cui, Q.; Baboul, A. G.; Clifford, S.; Cioslowski, J.; Stefanov, B. B.; Liu, G.; Liashenko, A.; Piskorz, P.; Komaromi, I.; Martin, R. L.; Fox, D. J.; Keith, T.; Al-Laham, M. A.; Peng, C. Y.; Nanayakkara, A.; Challacombe, M.; Gill, P. M. W.; Johnson, B.; Chen, W.; Wong, M. W.; Gonzalez, C.; Pople, J. A. *Gaussian 03*, revision C.02; Gaussian, Inc., Wallingford, CT, 2004.

(17) Adamo, C.; Barone, V. *J. Chem. Phys.* **1998**, *108*, 664.

(18) Hurley, M. M.; Pacios, L. F.; Christiansen, P. A.; Ross, R. B.; Ermler, W. C. *J. Chem. Phys.* **1986**, *84*, 6840.
(19) Dunning, T. H. *J. Chem. Phys.* **1971**, *55*, 716.
(20) Dunning, T. H. *J. Chem. Phys.* **1970**, *53*, 2823.
(21) Lundin, A.; Panas, I.; Ahlberg, E. *J. Phys. Chem. A* **2007**, *111*, 9080.
(22) Tomasi, J.; Mennuci, B.; Cammi, R. *Chem. Rev.* **2005**, *105*, 2999.
(23) Ritchey, J. A.; Davis, B. M.; Pleban, P. A.; Bayse, C. A. *Org. Biol. Chem.* **2005**, *3*, 4337.
(24) Bayse, C. A.; Allison, B. A. *J. Mol. Model.* **2007**, *13*, 47.
(25) Bayse, C. A.; Baker, R. A.; Ortwine, K. N. *Inorg. Chim. Acta* **2005**, *358*, 3849, and references therein.
(26) Fischer, H.; Dereu, N. *Bull. Soc. Chim. Belg.* **1987**, *96*, 757.
(27) Sarma, B. K.; Mugesh, G. *Chem.—Eur. J.* **2008**, *14*, 10603.
(28) Morgenstern, R.; Cotgreave, I. A.; Engman, L. *Chem.−Biol. Interact.* **1992**, *84*, 77.
(29) Sarma, B. K.; Mugesh, G. *J. Am. Chem. Soc.* **2005**, *127*, 11477.
(30) Bhabak, K. P.; Mugesh, G. *Chem.—Eur. J.* **2007**, *13*, 4594.

JP901880N